

Interpretation of the Source Saturn Ring Profile

Mark R. Showalter
PDS Rings Node
December 21, 2002

This report describes a thorough analysis of the timing and calibration of the Saturn ring profile, provided as one of the source files in this data set. See SORCDATA/DELSCO1.TXT for the original file.

This file was provided to the Rings Node by Padma Yanamandra-Fisher of JPL in 1993. It is similar to another file held by Philip Nicholson of Cornell at about the same time. The origin of the file is uncertain but it clearly contains the careful processing and calibration of the data set initially performed by Jay Holberg of U. Arizona from the early 1980's.

Unfortunately, much of Holberg's work was never carefully documented and most of the intermediate steps between this highly processed file and the original raw data (in SORCDATA/DELSCO.VOY) have been forgotten.

This document describes the process whereby I was able to recover many of the lost processing steps, which are now preserved in this archive.

(1) Background Information

This message from Padma Yanamandra-Fisher describes the three columns of SORCDATA/DELSCO1.TXT.

```
>From: JPLSC8::PADMA      19-MAR-1993 09:06:22.17
>To:   GAL::SHOWALTER
>CC:   PADMA
>Subj: SAT UVS Data
>
>Hi, Mark,
>The next file I shall send to you will contain the UVS occultation
>data at Saturn. The format of the records is as follows:
> Orbital distance from Sat  Opacity(tau)  Parameter E
> (km)
>
>Parameter E is an estimate of the error in the photon counts at that
>location and can be used to compute +/- 1 sigma.
>
>...
>
>Thanks,
```

Padma

A similar definition of parameter E was also provided by Bill Sandel.

Program DELSCO01.FOR was used to convert SORCDATA/DELSCO1.TXT into DELSCO1.TAB, which contains the same numbers but is in the standard format for a PDS table.

The values of tau (column #2) and E parameter (column #3) are plotted as a function of radius (column #1) in Figures 1 and 2. See files

SPROFI01.PS and SPROFI02.PS. The former is a familiar-looking profile of Saturn's ring system. The latter shows large variations, related to the strong dependence of the UVS instrument's sensitivity on the location of the star within the field of view.

(2) Data Spacing

The first column of DELSCO1.TAB contains radius values in km. A plot of (radius[n+1] - radius[n]) versus radius (Figure 3; see file SPROFI03.PS) reveals that most radial steps are ~3 km but a few individual steps are twice as large. These clearly correspond to missing time steps. A file DELSCO2.TAB was created in which the missing records have been added, using tau = -1 and eparam = -1.

(3) FDS Time Tags

The raw FDS file SORCDATA/DELSCO.DAT has FDS time tags but DELSCO2.TAB does not. Now that any gaps have been filled in, we wish to identify which record in the raw file corresponds to which record in DELSCO2.TAB.

Program FULLSUM.FOR was run to create file FULLSUM.TAB, which contains full spectral sums (samples 1-126) vs. record number for all of the records in the edited data file EDITDATA/US1W01P.DAT.

In this file, it was eventually possible through trial and error to associate specific features in both files. For example, the Maxwell Ringlet is shown from DELSCO2.TAB in Fig. 4 (SPROFI04.PS) and from FULLSUM.TAB in Fig. 5 (SPROFI05.PS). In the former figure, points are plotted versus radius and every tenth point is labeled with its line number from the file. In the latter figure, points are plotted versus their record number. This illustrates that the record numbers differ by exactly 5100, meaning that the first record in DELSCO2.TAB corresponds to record number 5101 in FULLSUM.TAB. The corresponding FDS tag of the first record is 44001:26:001.

Program DELSCO3.FOR was used to write DELSCO3.TAB, which contains the three columns but has additional columns for record number, full spectral sum and FDS count.

(4) E Parameter Interpretation

A comparison of Figs. 4 and 5 reveals that the E parameter is larger than the full spectral sum by approximately a factor of three. Through some background knowledge and a bit of experimentation, the E parameter has been found to equal:

$$E = 3 * (UVS_counts - background) \quad [1]$$

Support for this relationship comes from the fact that long swaths of the data show values of E that have exactly the same remainder when divided by three. This is consistent with the idea that the background value, whatever it is, varies slowly during the occultation.

The reason for the factor of three is uncertain, but appears to be related to the goal of converting from UVS counts to actual photon counts---Holberg et al. (1987, p. 180) reported that the instrument recorded ~2.5 counts per photon, at least for the Uranus encounter. However, if this was the goal, then the scale factor was applied incorrectly, because it should have been divided instead of multiplied!

(5) Sample Range and Background Estimates

Using the full spectral sum values of file FULLSUM.TAB in Equation [1] above, it quickly becomes apparent that the result is nonsense, because the implied background value changes radically from record to record. This is because the value for UVS_counts is not a full spectral sum---it includes only a subset of the 126 spectral samples.

It takes a bit of sleuthing to identify the range of samples were used to derive the E parameter. Program SUBRANGE.FOR examines every possible combination of starting index s1 and ending index s2 to see if any are consistent with the idea that the background value is a constant within the first twelve records of the file. The background is likely to be constant here because the first twelve values of E all have the same remainder when divided by three.

A run of the program reveals that the sample range (s1=31, s2=120) is the UNIQUE subrange consistent with this requirement. Although this result was based on only 12 samples, it becomes apparent in the analysis to follow that this exact range of samples was summed by the UVS team throughout their calibrated data file---if this had not been the case, then the derived background and stellar count values would show many additional anomalies.

Program DELSCO4.FOR writes out file DELSCO4.TAB, which is identical to file DELSCO3.TAB except that the column of full spectral sums has been replaced by two, one containing the sum of samples 31-120 and the next containing the background estimate, using formula [1] above.

(6) Data Gap

The fifth column of file DELSCO4.TAB contains -1 wherever the corresponding spectrum in file EDITDATA/US1W01P.DAT is empty. It is a bit surprising that DELSCO4.TAB shows a gap from records 10291 to 10305 (FDS 44002:00:091-105) even though the E parameter looks perfectly reasonable. This suggests that the UVS team had access to data records that were subsequently lost from the files obtained by the Rings Node. Although we cannot replace the lost spectra, we now have enough information to replace the missing spectral sums.

Before and after this set of records, the background has a fixed value of 29. It is reasonable to assume that it is 29 for the missing records as well. If so, then we can invert [1] to solve for UVS_counts:

$$\text{UVS_counts} = E/3 + 29 \quad [2]$$

Program DELSCO5.FOR creates a new file DELSCO5.TAB, which is identical to DELSCO4.TAB except that these records have been filled in.

(7) Background Model

The background model from DELSCO5.TAB is plotted in Fig. 6 (SPROFI06.PS). The ring profile is plotted across the bottom for comparison. The figure shows that the background is "jittery", owing to the fact that it has been derived from E parameters that were rounded to integers. Nevertheless, it is also clear that a simple model, consisting of 11 individual straight line segments, was originally used to describe the background variations. Estimated locations of the 12 breakpoints between the individual segments are marked as open circles in the figure.

A single bad background point is visible at record number 16241. This is most likely explained by a discrepancy between the raw data used for this investigation and that used for the original analysis. This point has been replaced by -1 in file DELSCO6.TAB, which is otherwise identical to DELSCO5.TAB.

A simplified background model has been generated by fitting straight lines to the individual segments shown in the plot. This has been accomplished by looking at the locations on each side of each breakpoint where the background jumps by 0.333. The midpoint of these jumps is the closest approximation to the actual location of the original background model, before it was converted to integer multiples of 1/3. These points have been tabulated in program SBACK1.FOR. Running this program generates SBACK1.TAB, which contains the smoothed model. The output of this program lists the derived coordinates of all 12 breakpoints:

No	Record Number	Background Counts
1	5100.500000000000	15.33333333333333
2	6291.625000000000	15.33333333333333
3	7948.500000000000	22.25862068965516
4	9723.05259259259	27.82148148148147
5	10396.44960918010	29.05934364432617
6	11333.53827072998	34.63103393968029
7	12724.14926590538	39.56978430306326
8	14142.04545454545	35.66666666666667
9	21683.37500000000	35.66666666666667
10	22824.50000000000	38.50000000000000
11	23523.71035598706	48.12531463502343
12	24416.50000000000	55.83333333333333

Figure 7 (SPROFI07.PS) provides a close-up comparison between the derived background values and the straight-line approximation.

(8) Stellar Count Estimates

The stellar counts can be derived by inverting the standard formula:

$$\text{counts} = \text{stellar} * \exp(-\text{tau}/\mu) + \text{back} \quad [3]$$

The value of $\mu = \sin(28.71)$ according to Holberg et al. (1982, p. 115).

Program DELSCO7.FOR reads DELSCO6.TAB and inserts a column containing the derived stellar count value, yielding DELSCO7.TAB. Although Eq. [3] can be solved in general, experimentation reveals that the estimate is very noisy whenever E is less than 10-20. We have adopted a cutoff of 12, such that the stellar counts are set to -1 wherever $E \leq 12$. Figure 8 (SPROFI08.PS) shows the results, with the ring profile included across the bottom for comparison.

This table shows very large variations in the stellar count value. This arose from the "limit cycle" motion of the Voyager spacecraft. Voyager was designed to keep point the spacecraft to a certain level of tolerance, called the limit cycle. Unfortunately, that tolerance was a bit larger than narrow width of the UVS slit. As a result, small changes in spacecraft orientation could result in substantial changes to the brightness of the star in the UVS instrument. These large variations are apparent in the data.

One question that could be asked in advance is whether the best background value to use for this purpose is the smoothed one in SBACK1.TAB or the "jittery" one in DELSCO6.TAB. It depends on whether the rounding to integer was performed before or after the value of tau was determined. In fact, the roundoff appears to have occurred first, because Fig. 8 shows no trace of the jitters that are present in Figs. 6 and 7.

Gaps in the plot appear wherever the stellar counts could not be derived. These gaps are most prevalent in the C Ring, where the opacity (optical depth) is high so the value of the E parameter frequently falls below the cutoff value of 12. The smaller values of E also explain the increase in noise within these regions. Nevertheless, it will be straightforward to smooth and interpolate to obtain a trustworthy model for the stellar counts throughout this region.

(9) A Ring Anomaly, Part I

A puzzling feature of Fig. 8 is the local increase in noise in the central A Ring, around records 22000-23000. Figure 9 (SPROFI09.PS) shows a close-up of this region, with the ring profile plotted along the bottom for comparison. Clearly, here the derived stellar count rate is closely correlated with the opacity. The Encke Gap and several density and bending waves are apparent in the stellar counts. This cannot be real. Note that this effect is not observed anywhere else in the ring system.

There are a number of possible explanations, all boiling down to an error in one of the terms of Eq. [3]:

$$\text{counts} = \text{stellar} * \exp(-\text{tau}/\mu) + \text{back}$$

An error in mu could cause this correlation, but it is difficult to imagine why the value of this constant could have varied while tau was being derived. A more plausible explanation is an offset in the background, which somehow got reflected in the tau calculation but not in the determination of the E parameter.

It is possible to solve [3] simultaneously for the stellar and background count rates by using several consecutive records in the file. For example, consider three consecutive samples:

$$\begin{aligned} \text{count1} &= S1 * \exp(-\text{tau1}/\mu) + B1 \\ \text{count2} &= S2 * \exp(-\text{tau2}/\mu) + B2 \\ \text{count3} &= S3 * \exp(-\text{tau3}/\mu) + B3 \end{aligned} \quad [4]$$

Here the unknowns are the stellar count rates S1, S2 and S3, and the background values B1, B2 and B3. Let us make the following assumptions:

(a) The stellar count rate is changing linearly, so that

$$S1 + S3 = 2*S2 \quad [5]$$

(b) All three background values have the same offset X from the previously derived background values, so that

$$\begin{aligned} B1 &= \text{back1} + X \\ B2 &= \text{back2} + X \\ B3 &= \text{back3} + X \end{aligned} \quad [6]$$

In effect, we are seeking a slowly-varying value for X, which we expect to be zero outside this particular region of the A Ring.

We now have seven equations with seven unknowns. We solve for X in a straightforward manner. First we solve [4] for S1, S2 and S3 and substitute them into [5], yielding:

$$(\text{count1} - B1)/\text{et1} + (\text{count3} - B3)/\text{et3} = 2*(\text{count2} - B2)/\text{et2} \quad [7]$$

Here $et[j]$ is shorthand for $\exp(-\tau[j]/\mu)$.

Next, we substitute [6] into [7] and rearrange to solve for X:

$$X = (cb1/et1 - 2*cb2/et2 + cb3/et3) / (1/et1 - 2/et2 + 1/et3) \quad [8]$$

Here $cb[j]$ is shorthand for $(count[j] - back[j])$.

Program BACKFIT.FOR tabulates these values for sequential sets of three records throughout DELSCO7.TAB, yielding BACKFIT.TAB. In a first iteration, it became apparent that the value for X was very unreliable whenever the magnitude of the denominator in [8] was smaller than about 1. Hence, these solutions are excluded from the output file.

The results are shown in Fig. 10 (SPROFI10.PS). It demonstrates conclusively that a background correction is needed in the central A Ring (records 22000-23000) but not elsewhere in the ring system. The maximum correction is roughly three.

(10) A Ring Anomaly, Part II

Although Fig. 10 demonstrates the need for a localized correction, it does not appear to be accurate enough to determine the correction's optimal amplitude. For this purpose, I return to the notable features in the A Ring (Fig. 9). For each feature, I determine by experimentation the best value of X to suppress the feature.

Program XTEST.FOR is a variant on program DELSCO7.FOR, in which background values are uniformly shifted by a constant X before the stellar count rate is determined. Using the program, I have generated a suite of output files:

Filename	X value
XTEST0.TAB	0
XTEST1.TAB	1
XTEST2.TAB	2
XTEST3.TAB	3
XTEST4.TAB	4

For each feature, I plot all five curves and select the one that best suppresses the feature. As an example, Fig. 11 (SPROFI11.PS) shows the region around the Encke Gap, where values between 3 (blue curve) and 4 (violet curve) seem to work best.

Here is a summary of the results of this exercise:

Location (record)	Estimated X	Radius (km)	Feature
22060	0.9	130750	Janus 5:4 density wave
22410	2.0	131850	Mimas 5:3 bending wave
22590	2.7	132350	Mimas 5:3 density wave
22940	3.3	133400	Encke Gap inner edge
23050	2.7	133750	Encke Gap outer edge
23230	2.0	134300	Janus 6:5 density wave

Feature identifications are from Fig. 1 of Holberg et al. (1982).

These six points are plotted in Figure 12. It clearly shows that the data are consistent with a "triangle" function that reaches a peak of approximately 3.5. The points are surprisingly consistent given the qualitative nature of the measurements summarized above.

How could this error have arisen? It is worth noting that the background model is already composed of short line segments (Figs. 6 and 7). Furthermore, the vertical, dotted lines show the locations of the 9th, 10th and 11th breakpoints. Hence, it appears that the A Ring anomaly can be removed to high precision simply by shifting the 10th point upward by about 3.5. The solid line shows this model. While not the best fit to the data in the least-square sense, the line falls within a few tenths of each point, which is well within individual uncertainties. But best of all, this correction now looks like the sort of last-minute correction (or minor typo) that might have cropped into the data analysis.

Furthermore, the peak ordinate on this plot is not arbitrary. It was determined by the amount (3.589) that breakpoint #10 would need to be shifted upward to align it with the final line segment (connecting points #11 and #12). This seems to be a very plausible change, because it is equivalent to eliminating the 11th breakpoint and then adjusting the 10th point accordingly.

(11) Corrected Profile

Based on the discussion above, we proceed on the assumption that a shift to the background is called for within the A Ring. Program DELSCO8.FOR generates the file DELSCO8.TAB, with corrected calibration values. Also, program SBACK2.FOR generates file SBACK2.TAB, with the new linearized background model. Here are the coordinates of the breakpoints, as printed out by the program:

No	Record Number	Background Counts
1	5100.500000000000	15.33333333333333
2	6291.625000000000	15.33333333333333
3	7948.500000000000	22.25862068965516
4	9723.05259259259	27.82148148148147
5	10396.44960918010	29.05934364432617
6	11333.53827072998	34.63103393968029
7	12724.14926590538	39.56978430306326
8	14142.04545454545	35.66666666666667
9	21683.37500000000	35.66666666666667
10	22824.50000000000	42.08858858858859
11	23523.71035598706	48.12531463502343
12	24416.50000000000	55.83333333333333

Figure 13 (SPROFI13.PS) shows the region of the A Ring where anomalies had previously been present (cf. Fig. 9). The anomalies now are substantially suppressed, although not completely absent.

Figure 14 (SPROFI14.PS) shows the new background model, for comparison to the original (cf. Fig. 7).

Finally, DELSCO9.TAB contains the data of DELSCO8.TAB but with the remaining bad stellar count determinations replaced by -1. This data file is now suitable for interpolation and smoothing to obtain a reliable, continuous model for the stellar counts.

References

Holberg, J. B., W. T. Forrester, and J. J. Lissauer 1982.
Identification of resonance features within the rings of Saturn.
Nature 297, 115-120.

Holberg, J. B., P. D. Nicholson, R. G. French, and J. L. Elliot 1987.
Stellar occultation probes of the Uranian rings at 0.1 and 2.2
microns: A comparison of Voyager UVS and Earth-based results. *Astron.*
J. 94, 178-188.

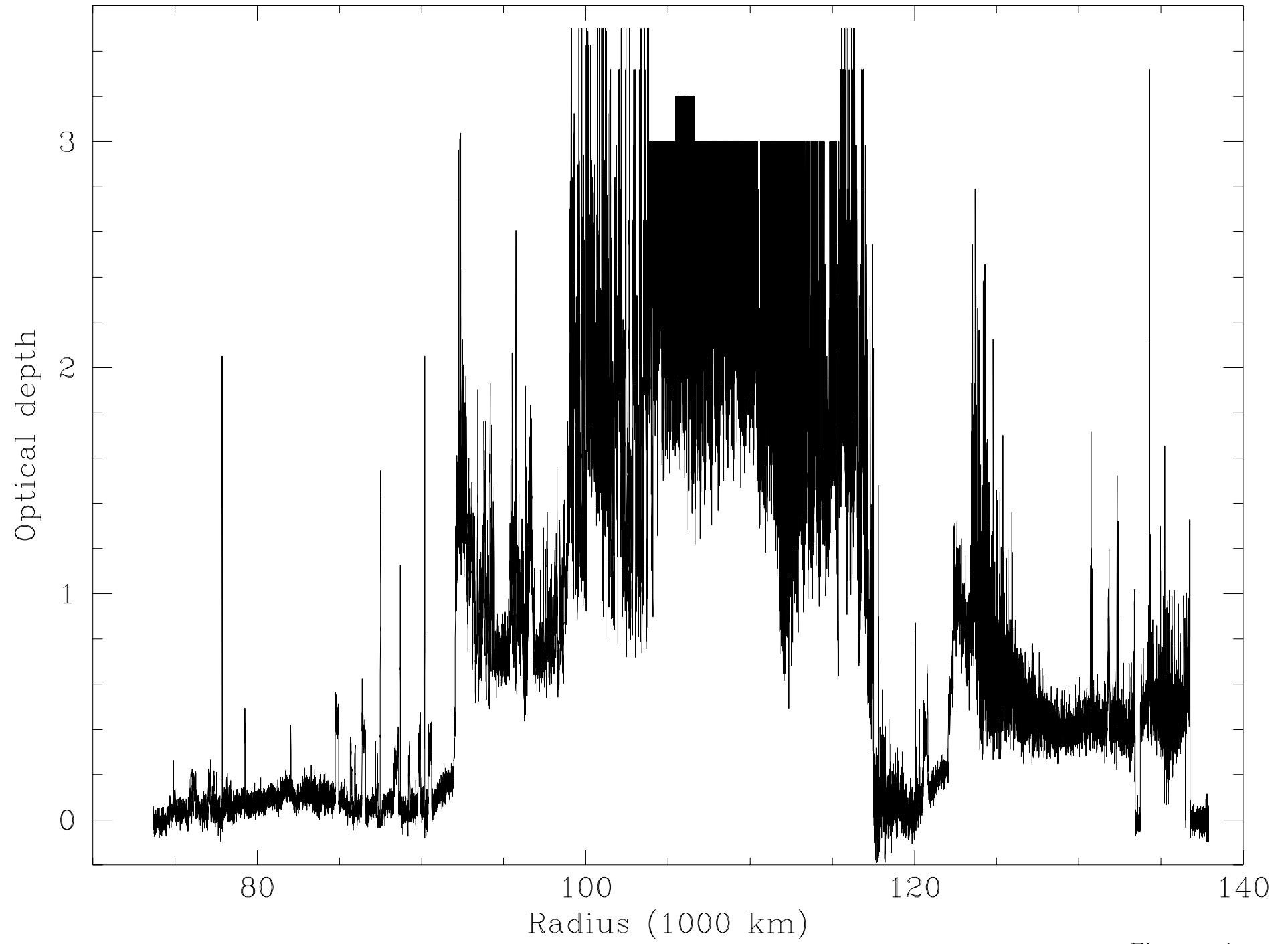


Figure 1.

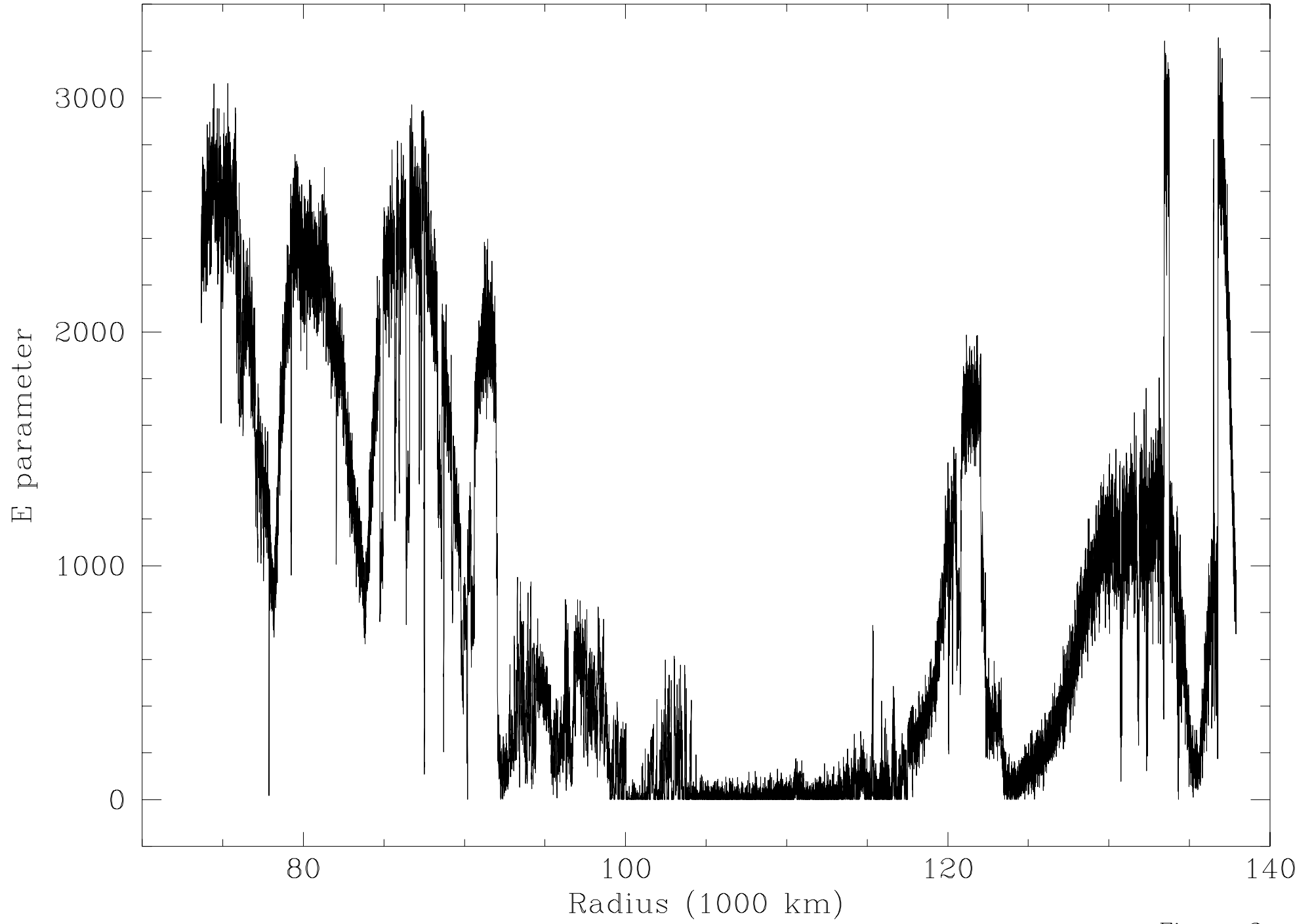


Figure 2.

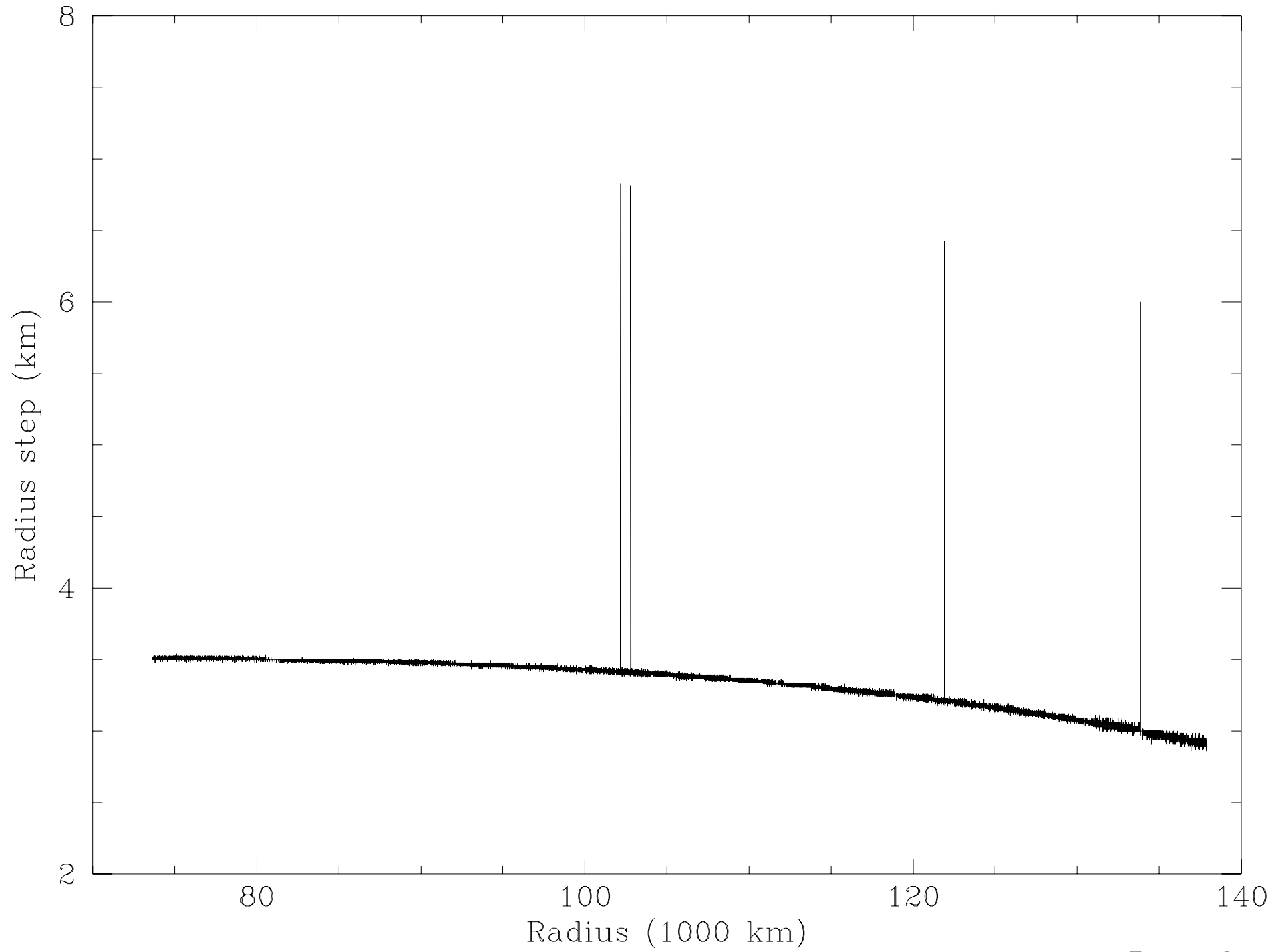


Figure 3.

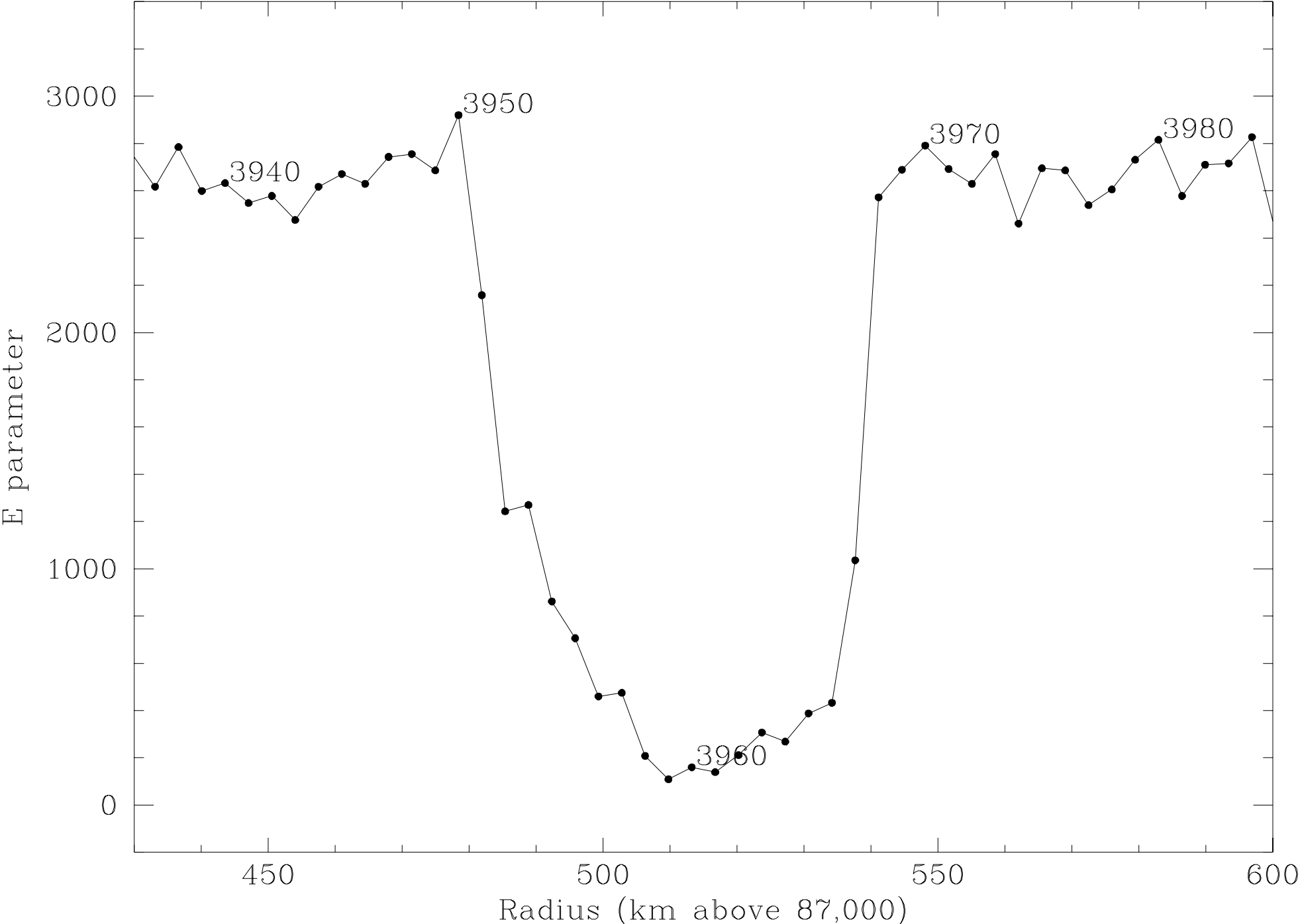


Figure 4.

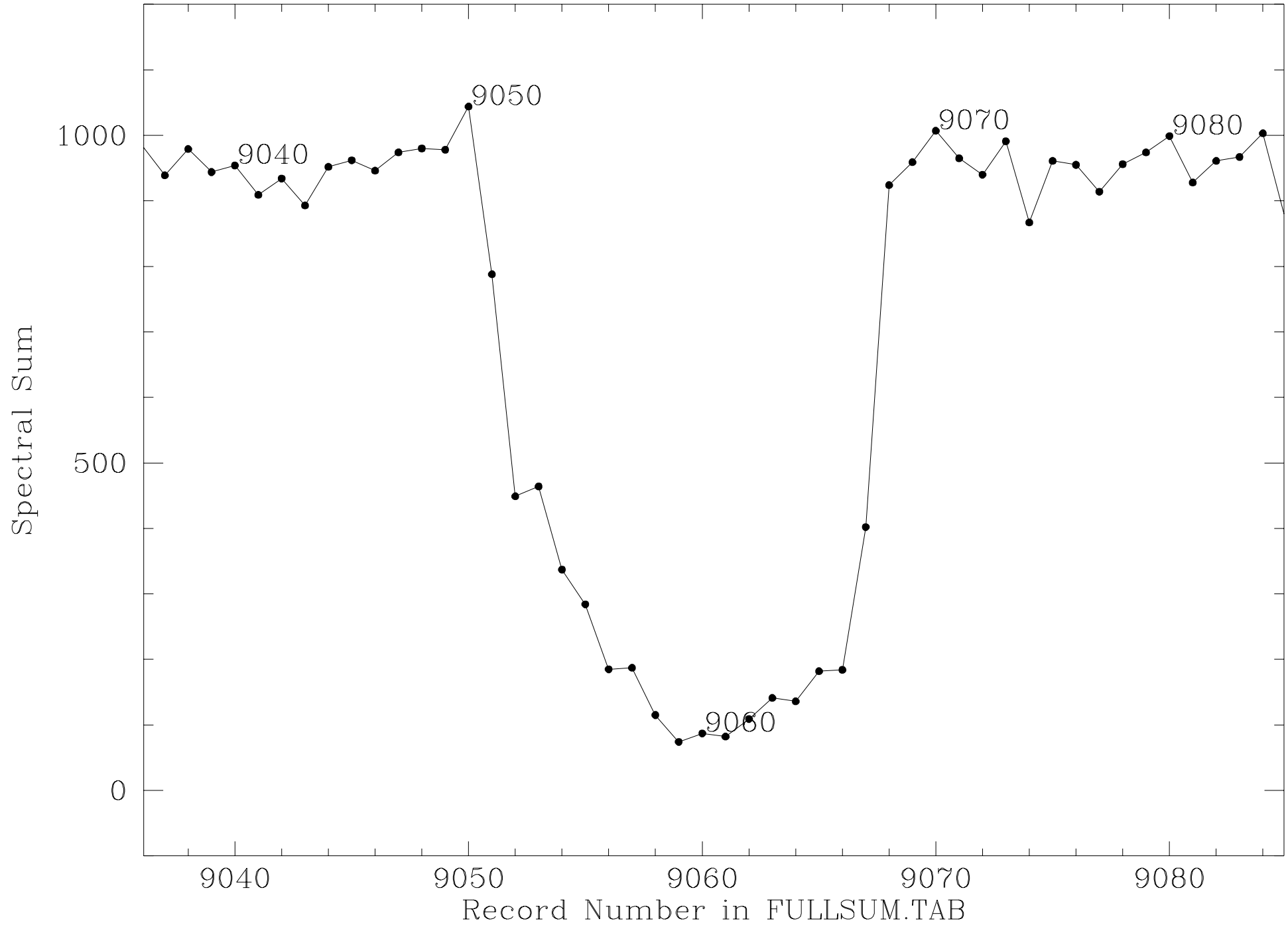


Figure 5.

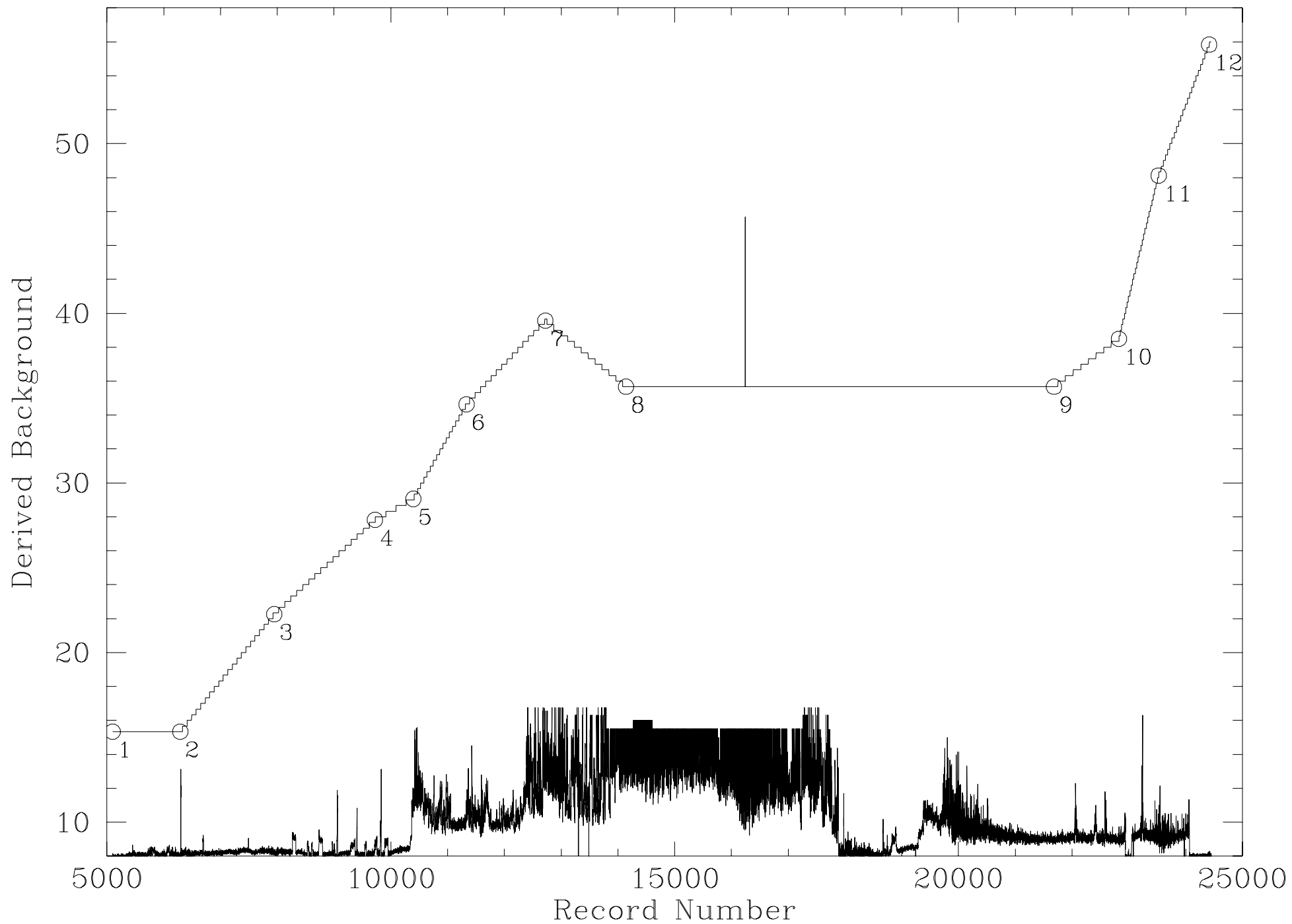


Figure 6.

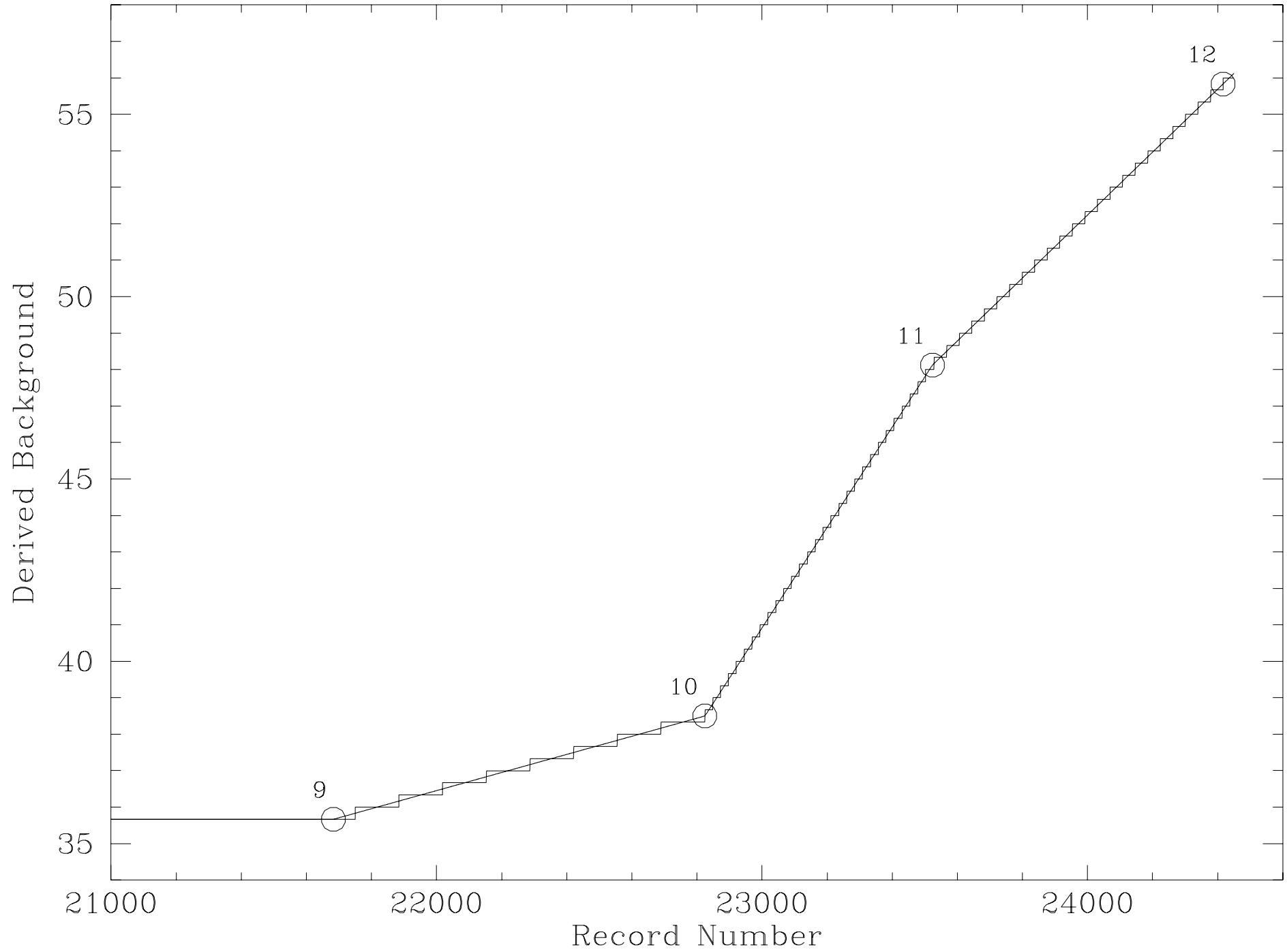


Figure 7.

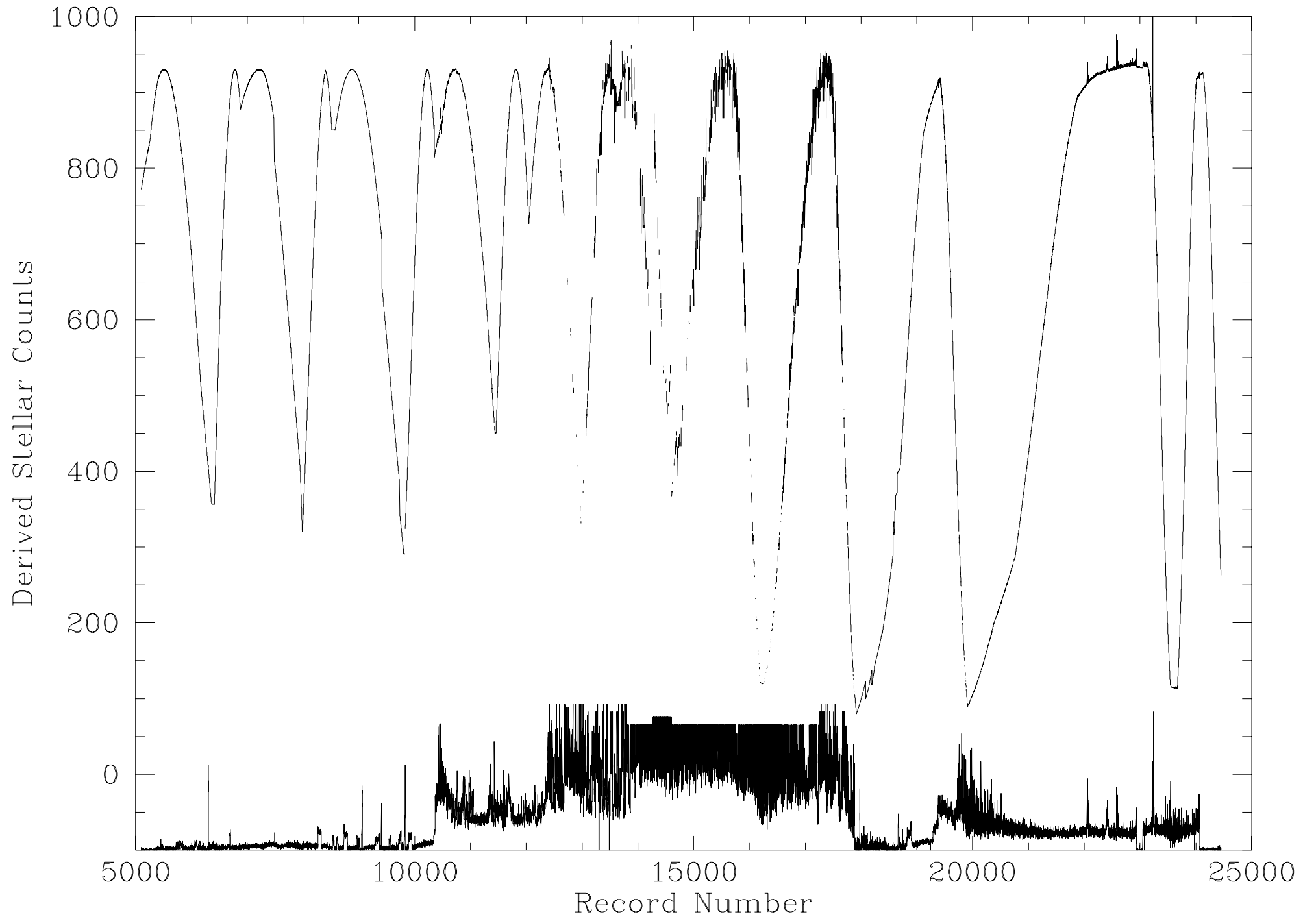


Figure 8.

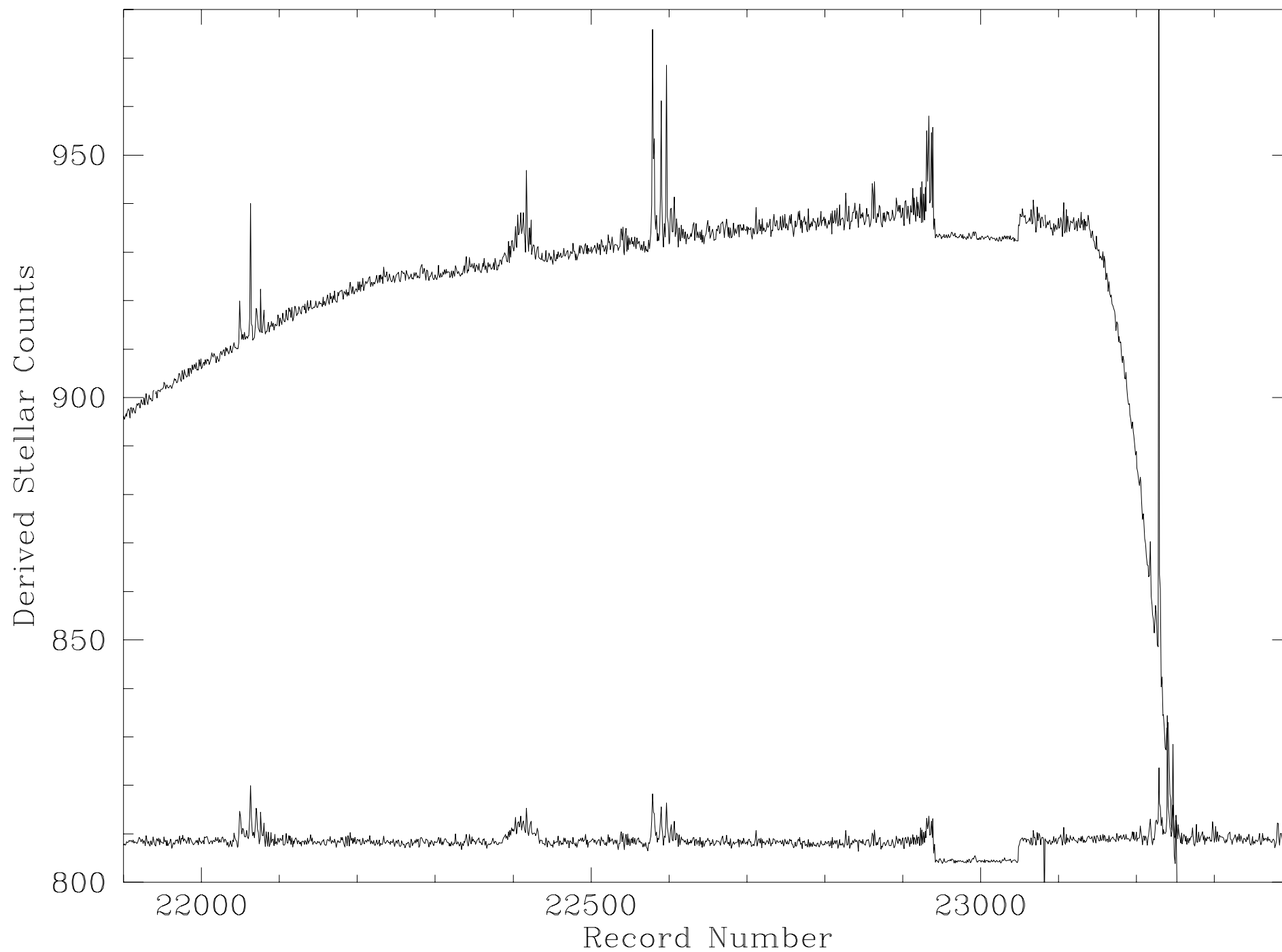


Figure 9.

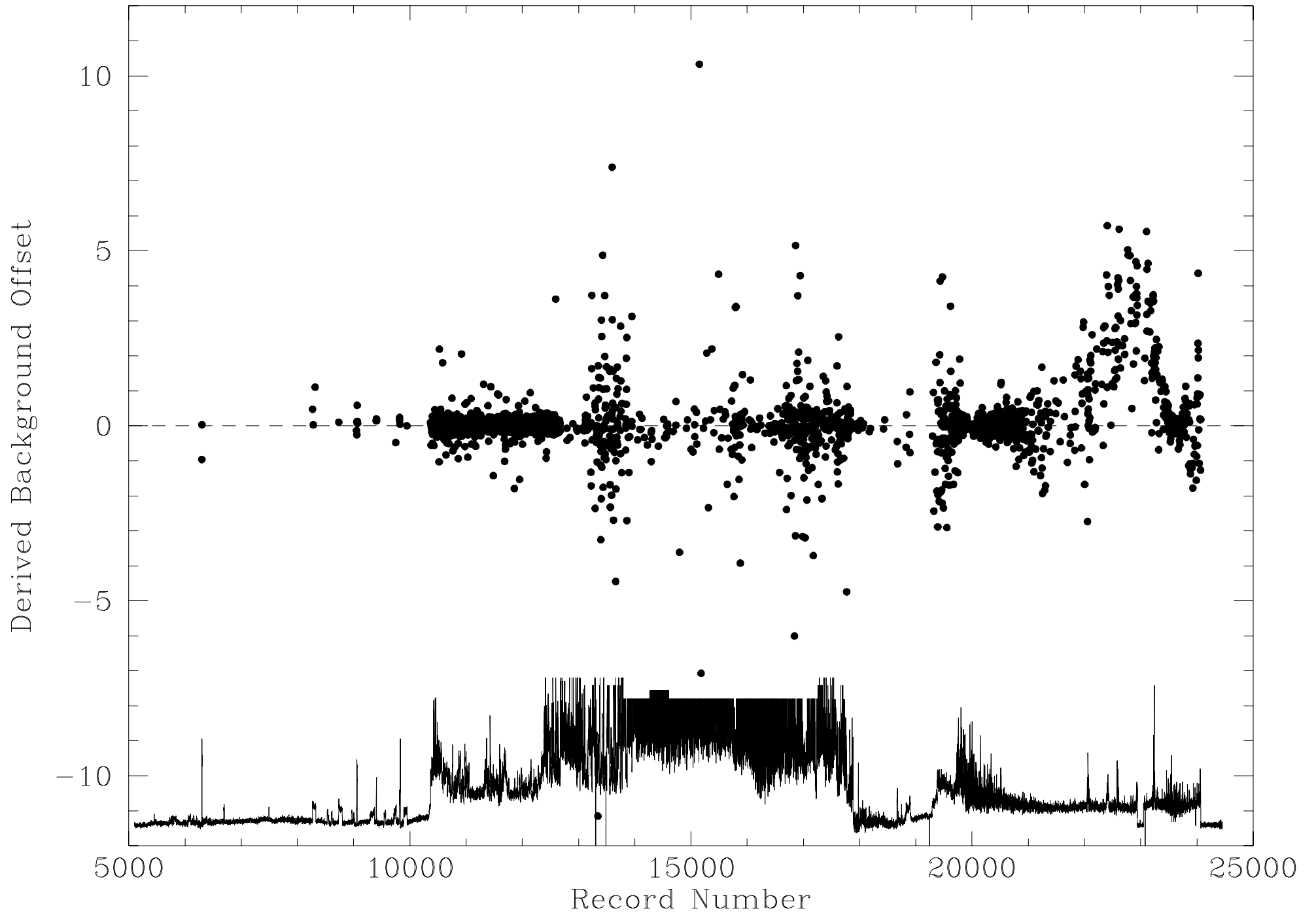


Figure 10.

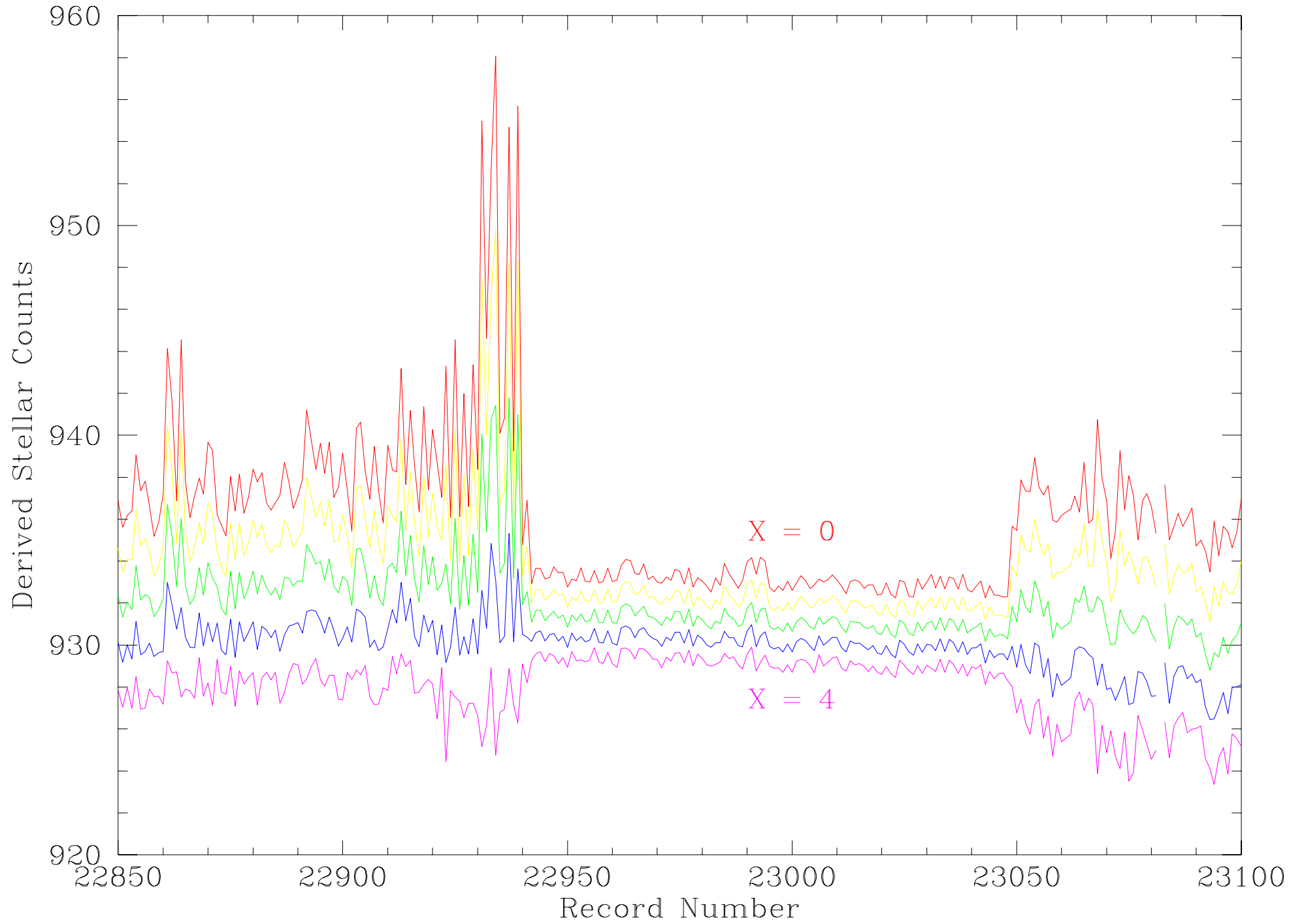


Figure 11.

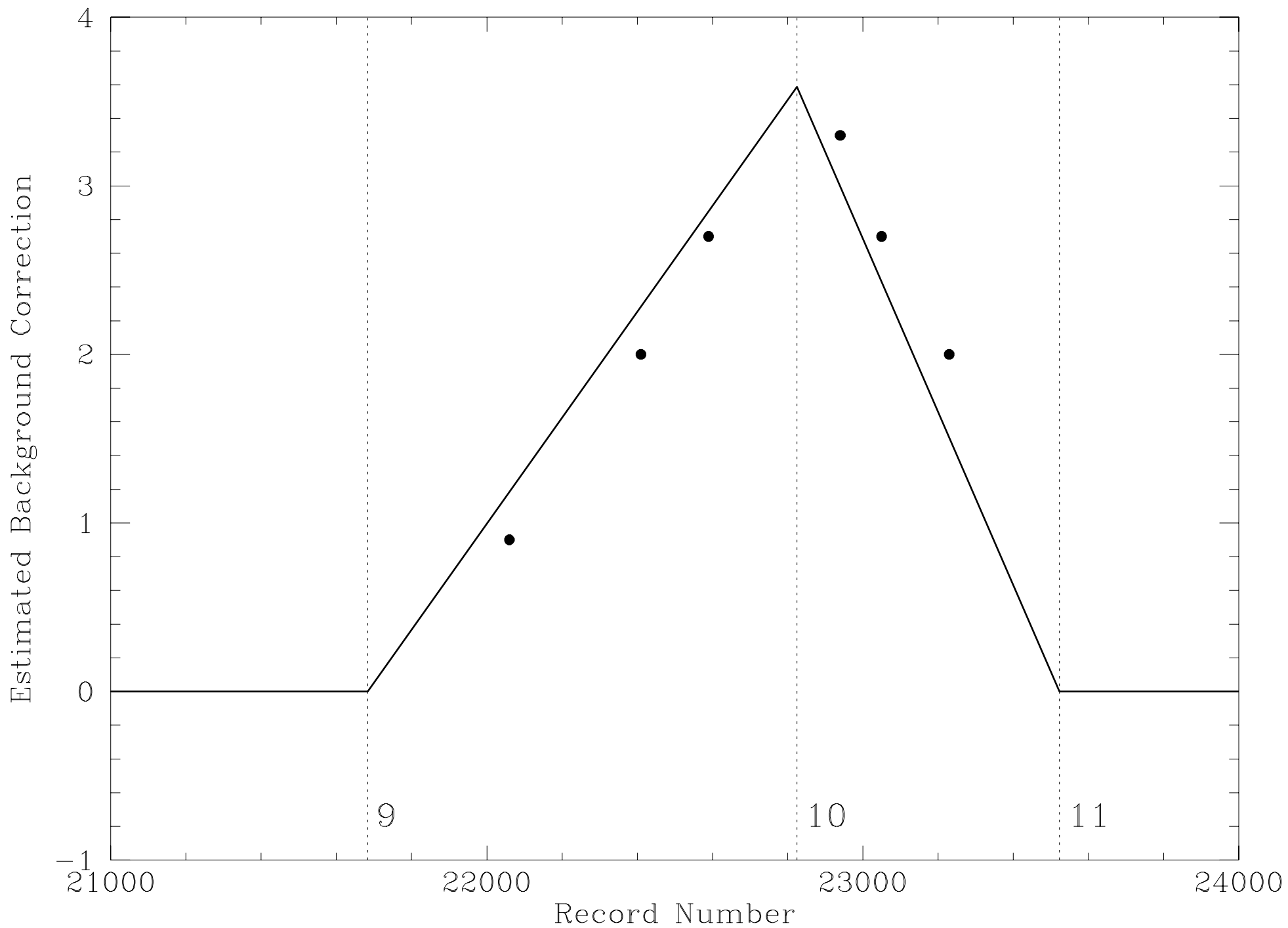


Figure 12.

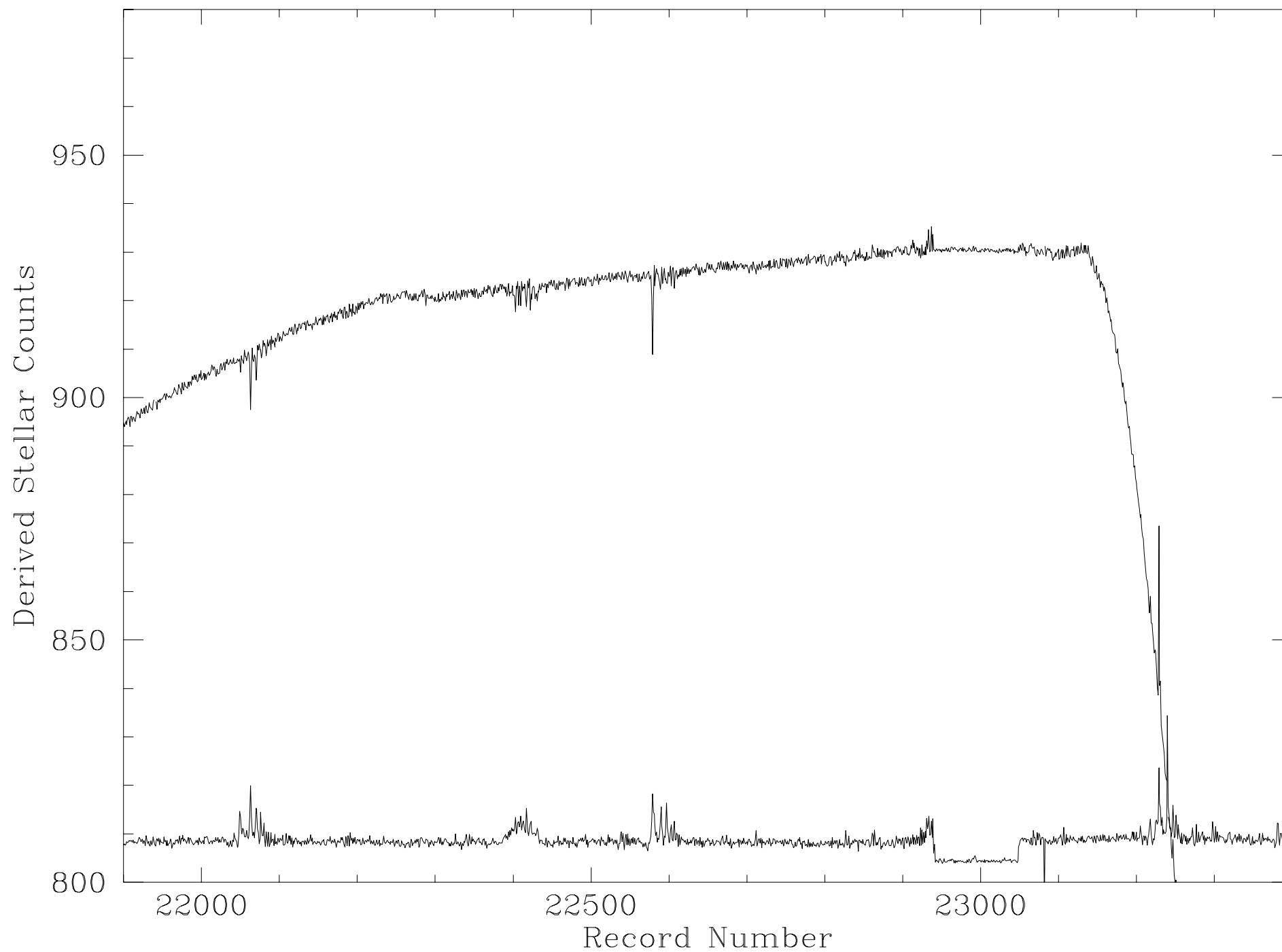


Figure 13.

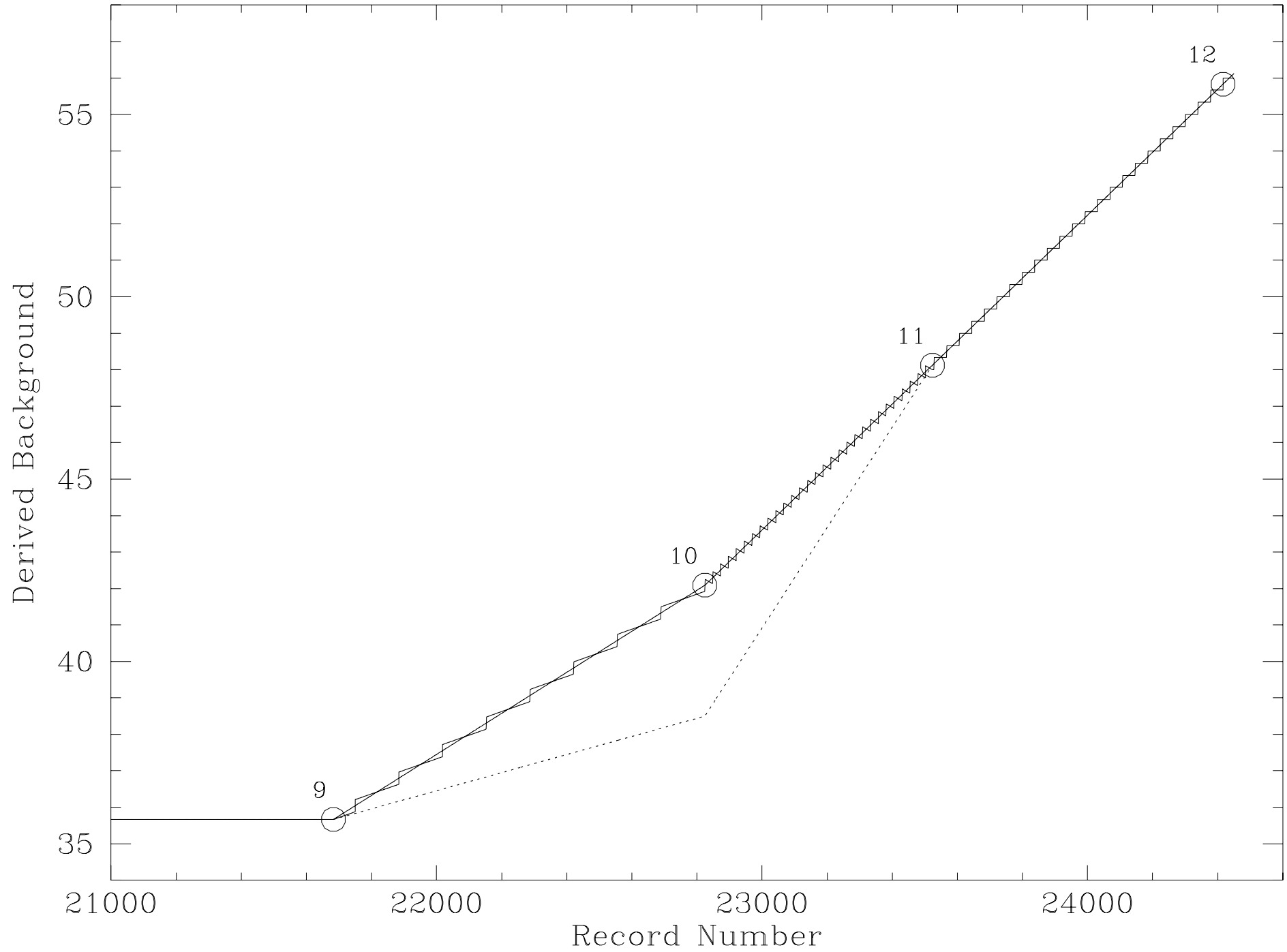


Figure 14.